Sparse Super-Resolution with Space Matching Pursuits

Guoshen YU and Stéphane MALLAT
CMAP, Ecole Polytechnique, 91128 Palaiseau Cedex, France

***Abstract*—Super-resolution image zooming is possible when the image has some geometric regularity. Directional interpolation algorithms are used in industry, with ad-hoc regularity measurements. Sparse signal decompositions in dictionaries of curvelets or bandlets find indirectly the directions of regularity by optimizing the sparsity. However, super-resolution interpolations in such dictionaries do not outperform cubic spline interpolations. It is necessary to further constraint the sparse representation, which is done through projections over structured vector spaces. A space matching pursuit algorithm is introduced to compute image decompositions over spaces of bandlets, from which a super-resolution image zooming is derived. Numerical experiments illustrate the efficiency of this super-resolution procedure compared to cubic spline interpolations.**

I. INTRODUCTION

Zooming operators that increase the size of images are often needed for digital display of images or videos. When images are aliased, linear interpolations [11] introduce artifacts such as Gibbs oscillations or zigzag along edges, and restore a blurred image. Better images can be estimated with super-resolution procedures which take advantage of this aliasing together with some geometric image properties.

A super-resolution algorithm computes a signal estimation in a space of dimension larger than the input signal size. Super-resolution algorithms are necessarily non-linear and can recover high frequency information by taking advantage of prior signal information. Super-resolution zooming algorithms are possible by interpolating the image along directions for which it is geometrically regular. Directional interpolations, usually known as edge-directed or content-adaptive interpolation, interpolate along directions that are computed with ad-hoc directional regularity estimations [8], [13]. These algorithms are used in industry with good numerical results.

If a signal has a sparse representation in a dictionary then a super-resolution estimation may be computed from lower-resolution measurements, if the dictionary is sufficiently *incoherent*. This approach has been used successfully for seismic sparse spike inversion or image inpainting [4], [5], [9]. Geometrically regular images have a sparse representation in curvelet [2], [1] or bandlet [7], [6], [10] dictionaries. However, subsampling a curvelet or a bandlets dictionary does not define a sufficiently incoherent dictionary to recover sparse super-resolution estimations for image zooming.

This paper introduces a super-resolution algorithm which computes structured sparse representations by projecting the image over selected bandlet vectors spaces. For super-resolution interpolation, this algorithm takes better advantage of prior image information by selecting vector spaces as opposed to individual vectors, which also reduces the computational complexity. These vector spaces are selected with a cascade of space matching pursuit algorithms. Directional interpolations derived from this sparse representation yields a super-resolution image estimation.

The paper first relates directional interpolations to super-resolution image zooming and reviews sparse super-resolution approaches. Section III introduces structured sparse representations by selecting vector spaces with matching pursuit algorithms. A super-resolution interpolation is derived, and numerical experiments provide comparisons with cubic spline interpolations.

II. DIRECTIONAL INTERPOLATION AND SPARSITY

A. Directional Interpolation

Let $f[n]$ be a high-resolution image whose frequency support is in $[-\pi,\pi]^2$. The measured low-resolution image y is obtained from a subsampling of f

$$y[n_1,n_2] = f[Kn_1,Kn_2] + w[n_1,n_2], \tag{1}$$

where w models the noise and $K > 1$ is the subsampling factor. In the following we assume $K = 2$ for simplicity. An image zooming computes an estimate $\tilde{f}$ of f from y.

If $w = 0$, the Fourier transform $\hat{y}$ of y is related to the Fourier transform $\hat{f}$ of f by

$$\hat{y}(\omega_1,\omega_2) = \sum_{k_1=0,1}\sum_{k_2=0,1} \hat{f}(\omega_1+k_1\pi,\omega_2+k_2\pi). \tag{2}$$

If y is free of aliasing, i.e., if the frequency support of f is included in $[-\pi/2,\pi/2]^2$ then a perfect reconstruction $\tilde{f} = f$ is obtained with a 2D linear sinc interpolation, which is a low-pass filtering:

$$\hat{\tilde{f}}(\omega_1,\omega_2) = \hat{y}(\omega_1,\omega_2)\,\hat{h}(\omega_1,\omega_2) = \hat{f}(\omega_1,\omega_2), \tag{3}$$

with $\hat{h}(\omega_1,\omega_2) = \begin{cases} 1 & (\omega_1,\omega_2) \in [-\pi/2,\pi/2]^2 \\ 0 & \text{otherwise} \end{cases}$.

If the frequency support of $\hat{f}$ exceeds $[-\pi/2,\pi/2]^2$, which is most often the case then y is aliased and (3) does no hold anymore. Any 2D linear interpolation introduces errors that result in artifacts such as Gibbs oscillations, blur and zigzag patterns along contours, as shown in Fig. 1(d). The ideal low pass filter h is generally replaced by a cubic spline interpolation filter which reduces artifacts. If the image has some directional regularity, it is possible to improve this

estimation and recover signal frequencies higher than $\pi/2$ by interpolating the image in the appropriate direction. Indeed, if the image is locally regular in a direction θ then its local Fourier transform has a narrow low-pass frequency support along this direction θ. Fig. 1(a) gives a simple illustration with a straight edge of direction θ whose Fourier transform is elongated in the direction $\theta + \pi/2$. Observe that if the low-pass filter h is replaced by a directional interpolator h_θ whose Fourier transform has a support in the elongated ellipsoid illustrated in Fig. 1(b) then it recovers an estimation $\tilde{f}$ whose Fourier transform in Fig. 1(c) satisfies

$$\hat{\tilde{f}}(\omega_1, \omega_2) = \hat{y}(\omega_1, \omega_2)\, \hat{h}_\theta(\omega_1, \omega_2) \approx \hat{f}(\omega_1, \omega_2), \qquad (4)$$

and thus achieves an almost perfect reconstruction by eliminating the aliased components. If $\theta = 0$ or $\theta = \pi/2$ then the support of $\hat{f}(\omega_1, \omega_2)$ and overlaps its aliased components and it is therefore not possible to separate them with a filter. In this case, no super-resolution is possible and the interpolation is implemented with a low-pass filter h.

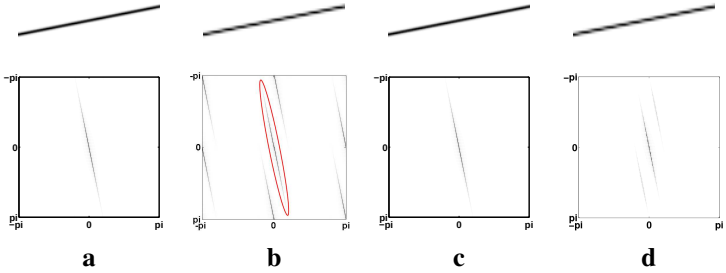

Fig. 1. (a): high-resolution edge image $f[n]$ and its Fourier transform. (b): a low-resolution image $y[n] = f[2n]$ and its aliased Fourier transform. (c): super-resolution estimation with directional interpolation along the contour direction (72.72 dB). The ellipse gives the frequency support of the directional interpolator. (d): 2D cubic-spline interpolation (50.45 dB).

Adaptive interpolation algorithms finds locally if there exists a direction θ along which the image variations are more regular than other directions, in which case it performs the interpolation in this direction with the filter h_θ. For complex images, measuring the "best direction of regularity" is difficult. Ad-hoc algorithms have been developed to do so and are used in industry for non-linear image zooming.

B. From Directional Interpolation to Sparsity

If a signal f has some directional geometric regularity then it has a sparse representation in a dictionary $\mathcal{D} = \{g_p\}_{p\in\Gamma}$ of curvelets [2], [1] or bandlets [7], [6], [10]. Finding an appropriate direction of interpolation can be connected to sparse super-resolution estimation, although we shall see that this sparse super-resolution estimation may not perform well for image interpolation. In the following we shall concentrate on a dictionary of curvelets but the same conclusions apply to a bandlet dictionary. A curvelet is an elongated oscillatory waveform whose Fourier transform is concentrated along a particular direction of the Fourier plane, as illustrated in Fig. 2. If f is an image with contours that are geometrically regular then it has a sparse representation in a curvelet dictionary. The signal f can thus be approximated by a small number $|\Lambda|$ of curvelets in a set Λ which specifies the directions, scales and positions of these curvelets

$$f = f_\Lambda + w_\Lambda \quad \text{with} \quad f_\Lambda = \sum_{p\in\Lambda} a[p]\, g_p. \qquad (5)$$

The approximation error w_Λ has a relatively small norm.

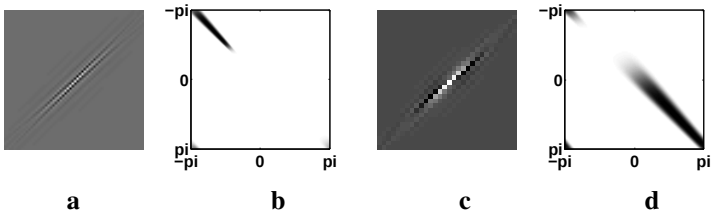

Fig. 2. (a): curvelet $g_p[n]$. (b): Fourier transform $\hat{g}_p(\omega)$. (c): subsampled curvelet Ug_p. (d): Aliased fourier transform $\widehat{Ug}_p(\omega)$.

Let us denote $y = Uf + w$ the low-resolution measurements where U is a subsampling operator. An estimation of f from y is computed by calculating an estimation of the sparse approximation support Λ of f in $\mathcal{D}$ [9] [4]. This is done by observing that y has a sparse representation with this same approximation support

$$y = \sum_{p\in\Lambda} a[p]\, Ug_p + w' \quad \text{with} \quad w' = Uw_\Lambda + w, \qquad (6)$$

in the subsampled dictionary

$$\mathcal{D}_U = \{Ug_p\}_{p\in\Gamma} \ . \qquad (7)$$

The approximation support Λ is estimated by computing a sparse approximation $\tilde{y}$ of y in $\mathcal{D}_U$

$$\tilde{y} = \sum_{p\in\tilde{\Lambda}} \tilde{a}[p]\, Ug_p \ , \qquad (8)$$

with an l^1 pursuit [3] or a matching pursuit [9]. A super-resolution estimation $\tilde{f}$ of f is derived by inverting U on the decomposition (8) of $\tilde{y}$. This is equivalent to applying an interpolation operator I_p to each subsampled Ug_p to recover g_p:

$$\tilde{f} = \sum_{p\in\tilde{\Lambda}} \tilde{a}[p]\, I_p(Ug_p) = \sum_{p\in\tilde{\Lambda}} \tilde{a}[p]\, g_p \ . \qquad (9)$$

This estimation can thus be interpreted as an adaptive interpolation of each Ug_p, and this adaptive interpolation is performed along the curvelet direction to recover the curvelet g_p. The estimated curvelet support $\tilde{\Lambda}$ defines the directions and supports of the interpolators that are used to compute $\tilde{f}$ from y.

The directional interpolation $\tilde{f}$ is an accurate estimation of f if the estimated support $\tilde{\Lambda}$ providing the regularity directions is an appropriate estimation of the approximation support Λ of f. The work of Tropp [12] shows that such a recovery is possible if the vectors in the transformed dictionary $\mathcal{D}_U = \{Ug_p\}_{p\in\Gamma}$ are highly incoherent. However

this condition does not hold for a dictionary obtained by subsampling curvelets on a uniform subgrid. Indeed, the finest scale curvelets g_p, which are responsible for high-frequency information restoration, when subsampled by the operator U, have no more vanishing moment and a relatively large energy at low frequencies. They therefore have a large correlation with other subsampled curvelets Ug_p at different scales and orientations. Since the dictionary $\mathcal{D}_U$ is highly redundant and not sufficiently incoherent, the computed support $\tilde{\Lambda}$ may be very different from the sparse approximation support Λ of f [12]. It leads to interpolation along inappropriate directions which introduces errors. As a result, on typical images, this type of super-resolution interpolation in curvelet dictionaries does not provide better results then cubic spline interpolations. The same conclusions applies when using a dictionary of bandlet vectors.

III. Structured Sparsity with Space Matching Pursuits

Observe in Fig. 1(b) that there is very little aliasing in the low-frequency square $[-\pi/2, \pi/2]^2$ of $\hat{y}(\omega)$. Errors introduced by linear interpolations are mostly concentrated at high frequencies. Let $\mathbf{W}$ be the space generated by the finest scale orthogonal wavelets along 3 orientations $\{\psi_n^k\}_{1\leq k\leq 3,n}$ and let $\mathbf{V}$ be the orthogonal complement corresponding to lower frequencies, generated by a family of orthogonal scaling functions $\{\phi_n\}_n$. To separate low and high frequencies, y is decomposed into

$$y = P_{\mathbf{W}}y + P_{\mathbf{V}}y = \sum_{k=1}^{3}\sum_{n}\langle y, \psi_n^k\rangle\, \psi_n^k + \sum_{n}\langle y, \phi_n\rangle\, \phi_n, \quad (10)$$

where $P_{\mathbf{W}}y$ is the orthogonal projection of y on $\mathbf{W}$ which carries the higher frequencies, and $P_{\mathbf{V}}y$ is the orthogonal projection over $\mathbf{V}$ corresponding to lower frequencies. Since $P_{\mathbf{V}}y$ is almost aliasing-free, it can be interpolated with a linear cubic-spline interpolator I_l. However, an optimized non-linear directional interpolation operator I_n is required to estimate the signal higher frequencies by interpolating $P_{\mathbf{W}}y$ while removing the aliasing:

$$\tilde{f} = I_n(P_{\mathbf{W}}y) + I_l(P_{\mathbf{V}}y). \quad (11)$$

A. Interpolations in Band Spaces

As explained in Sec. II, sparse super-resolution algorithms are highly flexible but suffer from this flexibility. In a curvelet dictionary, a signal is sparse if it is well approximated by a small number of curvelets, but there is no constraint on the properties of these curvelets. Recovering these curvelets from a subsampled signal requires a full search in a large dictionaries which leads to errors. Directional interpolations are much more constraint since locally all pixels are recovered by performing an interpolation with a single direction. To take advantage of this property, instead of decomposing the signal over dictionary vectors that are selected individually, a structured sparse super-resolution interpolation is computed by decomposing the signal over vector spaces selected from a dictionary $\{\mathbf{W}_b\}_{b\in\Gamma}$ of subspaces of $\mathbf{W}$. The chosen spaces provide a sparse image representation with a linear approximation within each space.

A wavelet band space $\mathbf{W}_b$ is generated by a family of finest scale wavelets $\{\psi_n^k\}_{1\leq k\leq 3,n\in b}$, where b is a directional band of B wavelets, for the three orientations $k = 1, 2, 3$, at the finest scale, as illustrated in Fig. 3. Bands have different directions and are translated to cover the image plane.

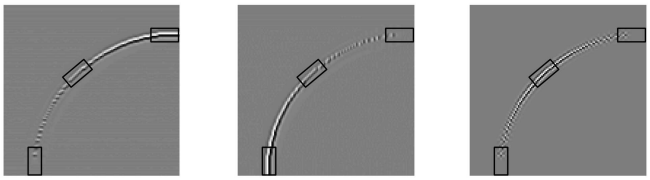

Fig. 3. A wavelet band space $\mathbf{W}_b$ corresponds to an oriented band of wavelet coefficients in the finest scale wavelet image coefficients for $k = 1, 2, 3$. The rectangles appear over the 3 wavelet orientations correspond to different band spaces.

The signal in $\mathbf{W}$ is decomposed as projections over a selected family of band spaces:

$$P_{\mathbf{W}}y = \sum_{b\in\Lambda} P_{\mathbf{W}_b}y. \quad (12)$$

The choice of band spaces $\{\mathbf{W}_b\}_{b\in\Lambda}$ is optimized to provide a sparse approximation. In each $\mathbf{W}_b$ there exists a bandlet basis providing a sparse linear approximation of $P_{\mathbf{W}_b}y$. To each band space $\mathbf{W}_b$ we shall associate an interpolator I_b which is a directional interpolation in the direction of the band if wavelet coefficients are indeed regular in this direction and a separable cubic spline interpolation otherwise

$$I_n(P_{\mathbf{W}}y) = \sum_{b\in\Lambda} I_b(P_{\mathbf{W}_b}y). \quad (13)$$

The resulting super-resulting estimator is

$$\tilde{f} = \sum_{b\in\Lambda}\sum_{k=1}^{3}\sum_{n\in B}\langle y, \psi_n^k\rangle\, I_b(\psi_n^k) + \sum_{n}\langle y, \phi_n\rangle\, I_l(\phi_n). \quad (14)$$

As opposed to (9), interpolators are chosen in blocks and not individually for each dictionary vector. Structuring the sparse signal decomposition with a predefined family of vector spaces takes advantage of prior information to reduce the search for a sparse signal decomposition, and hence the algorithm computational complexity. The choice of the band spaces $\mathbf{W}_b$ in (12) is regularized by first selecting locally the most appropriate angles in square neighborhoods and then finding the band locations for these angles. The local angle selection is performed with a space matching pursuit in a window Fourier domain, and the band locations is then computed with a matching pursuit over wavelet coefficients.

B. Window Fourier and Band Space Matching Pursuits

Appropriate band directions correspond to orientations along which the image is locally regular. If the image is regular in the direction θ then its subsampling has an energy concentrated in a frequency band of angle $\theta+\pi/2$ plus aliasing

components illustrated in Fig. 1(b). Directions of regularity in an image window can thus be identified by computing the energy concentration of a window Fourier transform along oriented frequency bands, which is implemented with a space matching pursuit.

The finest scale image components $P_{\mathbf{W}}y[n]$ are localized in square windows, by a multiplication with translated Hanning windows of 16×16 pixels. Let $s[n]$ be such a high frequency image window. The Fourier transform of $s[n]$ gives the window Fourier transform of $P_{\mathbf{W}}y$. Let $\mathbf{V}_\theta$ be the space of signals whose Fourier transform have a support in a band of angle θ as illustrated in Fig. 4. Bands of different directions are adjusted to the have same size. The directions of local regularity in $s[n]$ are obtained by finding the Fourier spaces $\mathbf{V}_\theta$ which absorb the maximum signal energy. These multiple directions are computed with a space matching pursuit over a dictionary of vector spaces $\{\mathbf{V}_\theta\}_{\theta\in\Theta}$ which selects a family of vector spaces that approximate efficiently the signal energy along a small number of directions. The set Θ is a uniform discretization of angles in $[0, \pi)$, over 32 angles. An orthogonal projection $P_{\mathbf{V}_\theta}s$ over a space $\mathbf{V}_\theta$ is obtained by restricting the Fourier transform of s to the corresponding frequency band.

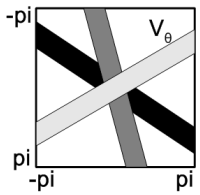

Fig. 4. Fourier vector spaces $\mathbf{V}_\theta$. Each band represents a Fourier vector space.

For any image square $s[n]$, the matching pursuit algorithm is initialized with $R^0 s = s$. At the step m, it selects the space $\mathbf{V}_{\theta_m}$ which yields the largest residual projection

$$\|P_{\mathbf{V}_{\theta_m}}(R^m s)\| = \max_{\theta\in\Theta} \|P_{\mathbf{V}_\theta}(R^m s)\|. \tag{15}$$

The next order residue is

$$R^{m+1}s = R^m s - P_{\mathbf{V}_{\theta_m}}(R^m s) \tag{16}$$

which yields a matching pursuit decomposition

$$s = \sum_{m=0}^{M-1} P_{\mathbf{V}_{\theta_m}}(R^m s) + R^M s \ . \tag{17}$$

One can verify that this matching pursuit is orthogonal because all spaces are generated by a block of vectors that belong to an orthogonal basis, in this case a Fourier basis. Selecting a family of spaces $\{\mathbf{V}_{\theta_m}\}_{0\le m<M}$ amounts to selecting a family of local directions $\{\theta_m\}_{0\le m<M}$ along which the image has some regularity. In numerical computations, M is typically between 3 and 5 over an image window of 16^2 pixels, and is thus much smaller than the total number of possible angles.

Once the M angles are selected, it is necessary to find the location of the bands b of angles θ_m which provide sparse image approximations. This means selecting a family of band spaces $\mathbf{W}_b$ among all bands having an orientations $\{\theta_m\}_{0\le m<M}$, at any location. The orthogonal projection $P_{\mathbf{W}_b}y$ is computed from the restriction of the wavelet coefficients of y in the band b. The selection of band spaces is performed with a matching pursuit which selects the bands which absorb the maximum signal energy. It is implemented with the space pursuit algorithm described (15)-(17) where the Fourier spaces $\mathbf{V}_\theta$ are replaced by wavelet band spaces $\mathbf{W}_b$, for bands having one of the M selected angles. The matching pursuit is also orthogonal because all spaces are generated by selecting blocks of vectors in a wavelet orthogonal basis. For the selected angles, this algorithm finds the positions of bands of wavelet coefficients having a maximum energy. The size of these bands are independent of their position and angle. The resulting band space matching pursuit over each image square $s[n]$ of $P_{\mathbf{W}}y$ yields the band space decomposition (12).

C. Bandlet Sparsity and Interpolations

A band space $\mathbf{W}_b$ is selected so that wavelet coefficients have a high energy variation within the corresponding band given that its angle is selected among local directions of regularity. To verify that wavelet coefficients are indeed regular in the band, we check that they have a sparse representation in a bandlet basis obtained by computing a directional wavelet transform of these wavelet coefficients [7], [6]. If it is indeed the case, then wavelet coefficients are interpolated along the band direction which is a direction of regularity. Otherwise, coefficients in the bands are interpolated with a cubic spline interpolation.

Bandlet coefficients in a band b of angle θ are computed by grouping pairs of neighbor wavelet coefficients $\langle y, \psi_n^k\rangle$ and $\langle y, \psi_{n'}^k\rangle$, such that $\vec{nn'}$ has an angle θ. For such each pair of coefficients, a Haar average and difference are calculated, which corresponds to bandlet coefficients

$$a_{nn'} = \frac{\langle y, \psi_n^k\rangle + \langle y, \psi_{n'}^k\rangle}{\sqrt{2}} \quad \text{and} \quad d_{nn'} = \frac{\langle y, \psi_n^k\rangle - \langle y, \psi_{n'}^k\rangle}{\sqrt{2}} \ .$$

If within a band, the sum of the squared difference coefficients is sufficiently small compared to the sum squared of wavelet coefficients in the band, then wavelet coefficients do have a regular variation along the direction θ of b. Wavelet coefficients in a band b are thus interpolated along this direction θ. Otherwise, if the regularity is not sufficient in the direction θ, a more conservative cubic spline interpolation is applied.

A directional interpolator I_b is applied to wavelet coefficients in a band b of angle θ, with a filter h_θ which must cancel the aliased components to satisfy (4). In the following, we describe such an interpolator for an image upscaling which multiplies by 2 the image rows and columns. It requires computing interpolations along two directions. A one-dimensional interpolation along θ provides accurate coefficient estimations if the image is regular in the direction of θ. The mid-point between any two points having an angle θ is calculated with such an interpolation. This will oversample by a factor two either the image rows, or the image columns or the diagonals

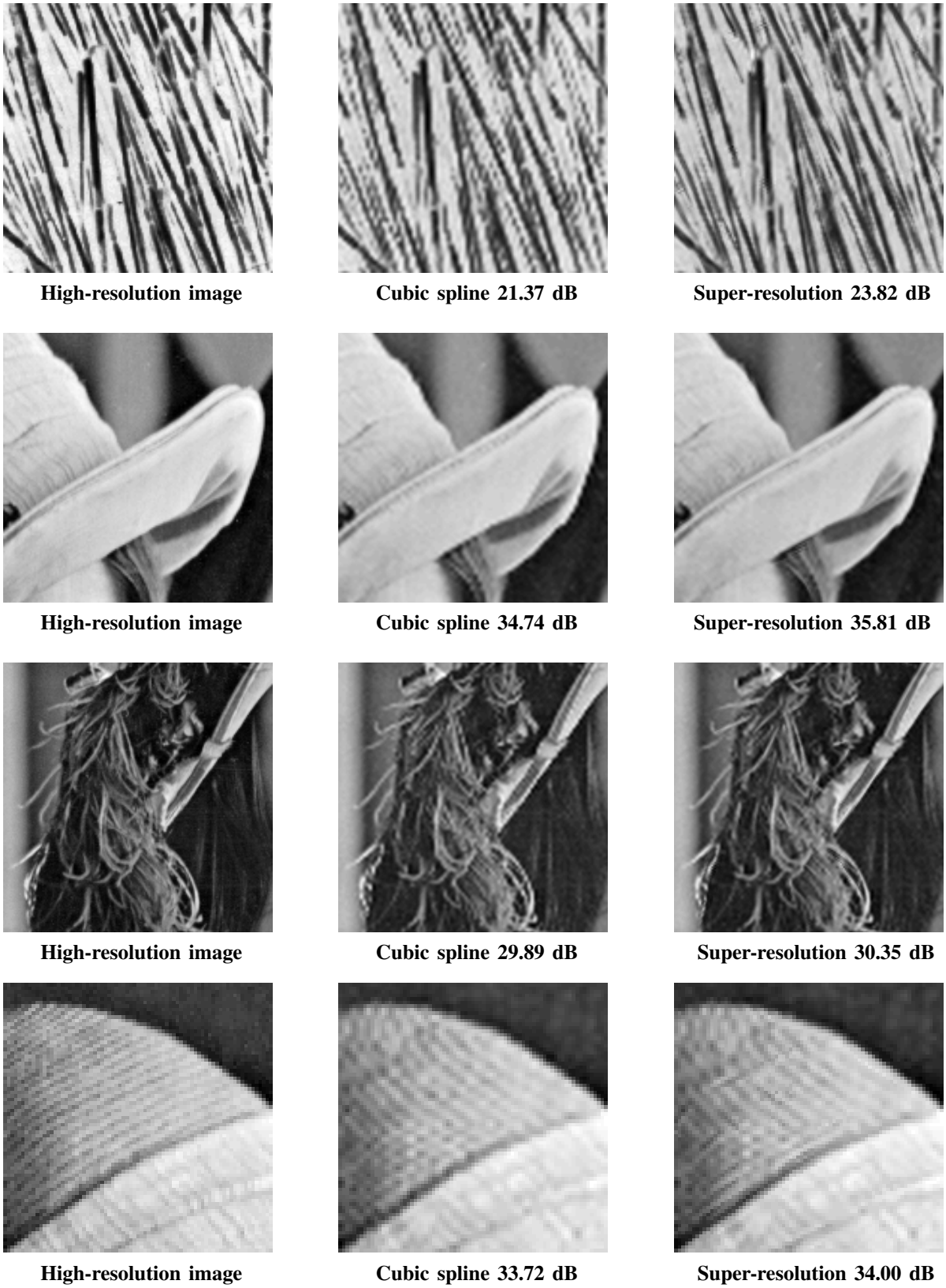

Fig. 5. From left to right: high-resolution image, cubic-spline interpolation, space matching pursuit super-resolution.

of angle $\pm\pi/4$. Along these oversampled rows, columns or diagonals, one can now compute a cubic spline interpolation with little aliasing error. These directions are interpolated to further increase the number of samples. The position of these new samples are chosen so that any missing upscaled image coefficient is in the middle of two new samples having a relative position of angle θ. These missing image coefficients are then computed with an interpolation along θ from new samples.

Fig. 6 illustrates this interpolation procedure with an example for $\theta = \arctan 1/2$. The subsampled grid shown with $\times$. The algorithm is decomposed in three steps.

1) Computation of the mid-point $\bigcirc$ between any two pair of samples having an angle θ, which are located along image columns for $\theta = \arctan 1/2$.
2) Interpolation along the oversampled image columns to compute new sample values $\bullet$.
3) Computation of the up-scaled image values at positions $\square$ by interpolating the new samples $\bullet$ along θ.

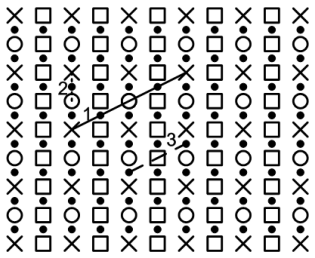

Fig. 6. Directional interpolation in three steps:a one-dimensional interpolations along angle θ, a vertical interpolation and another interpolation along θ.

Fig. 5 compares a separable cubic spline interpolation with a super-resolution interpolation computed with this super-resolution band space algorithm. The super-resolution achieves a significant PSNR improvement and improves the visual image quality where the image is geometrically regular. High-frequencies are restored along the direction regularity. This clearly appears in the straws, the hat border and the hairs of various directions. However, on the hat image at the bottom, because of Moiré effects, the windowed Fourier matching pursuit does not identify appropriate directions from the lower resolution hat image, and the super-resolution barely improves the cubic-spline result. When the image is too complex, the aliasing may destroy the directions of image regularity, in which case no super-resolution is achieved.

IV. Conclusion

Super-resolution with directional interpolations requires accurate estimation of the image directional regularity. We introduced an algorithm which computes directions of regularity by optimizing a structured sparse signal representation. This structured representation is computed by projecting the signal over vector spaces chosen from a dictionary, as opposed to a projection over individual vectors. It is computed with a cascade of space matching pursuits. This algorithm reduces the amount of computations compared to an optimization using individual dictionary vectors and provides more accurate super-resolution image estimations. When the image has regular geometric structures, the algorithm provides a better SNR and a better visual image quality than a cubic spline interpolation.

References

[1] E. Candes, L. Demanet, D. Donoho, and L. Ying. Fast Discrete Curvelet Transforms. *SIAM Journal of Multiscale Modeling and Simulation*, 5(3):861–899, 2006.

[2] E.J. Candes and D.L. Donoho. Curvelets: a surprisingly effective nonadaptive representation for objects with edges. Curves and Surfaces, 105–120. Edited by C. Rabut, A. Cohen, and LL Schumaker, 2000.

[3] S.S. Chen, D.L. Donoho, and M.A. Saunders. Atomic Decomposition by Basis Pursuit. *SIAM Journal on Scientific Computing*, 20:33–61, 1999.

[4] M. Elad, J.L. Starck, P. Querre, and D.L. Donoho. Simultaneous cartoon and texture image inpainting using morphological component analysis (MCA). *Appl. Comput. Harmon. Anal*, 19:340–358, 2005.

[5] MJ Fadili, J.L. Starck, and F. Murtagh. Inpainting and Zooming Using Sparse Representations. *The Computer Journal*, 2007.

[6] E. Le Pennec and S. Mallat. Bandelet Image Approximation and Compression. *SIAM Journal of Multiscale Modeling and Simulation*, 4(3):992–1039, 2005.

[7] E. Le Pennec and S. Mallat. Sparse geometric image representations with bandelets. *Image Processing, IEEE Transactions on*, 14(4):423–438, 2005.

[8] X. Li and MT Orchard. New edge-directed interpolation. *Image Processing, IEEE Transactions on*, 10(10):1521–1527, 2001.

[9] S. Mallat. *A Wavelet Tour of Signal Processing: The Sparse Way, 3rd edition*. Academic Press, 2008.

[10] S. Mallat and G. Peyre. Orthogonal bandelet bases for geometric image approximation. *Comm. Pure Appl. Math.*, 61(9):1173–1212, 2008.

[11] P. Thevenaz, T. Blu, and M. Unser. Interpolation revisited [medical images application]. *Medical Imaging, IEEE Transactions on*, 19(7):739–758, 2000.

[12] JA Tropp. Greed is good: algorithmic results for sparse approximation. *Information Theory, IEEE Transactions on*, 50(10):2231–2242, 2004.

[13] Q. Wang and RK Ward. A New Orientation-Adaptive Interpolation Method. *Image Processing, IEEE Transactions on*, 16(4):889–900, 2007.